

Article

Dynamics of Radiation Damage in AlN Ceramics under High-Dose Irradiation, Typical for the Processes of Swelling and Hydrogenation

Artem L. Kozlovskiy ^{1,2,*} , Dmitriy. I. Shlimas ^{1,2} , Inesh E. Kenzhina ^{1,2}, Daryn B. Borgekov ^{1,2} and Maxim V. Zdorovets ^{1,2,3} 

¹ Engineering Profile Laboratory, L.N. Gumilyov Eurasian National University, Nur-Sultan 010008, Kazakhstan; shlimas@mail.ru (D.I.S.); kenzhina@physics.kz (I.E.K.); borgekov@mail.ru (D.B.B.); mzdorovets@inp.kz (M.V.Z.)

² Laboratory of Solid State Physics, The Institute of Nuclear Physics, Almaty 050032, Kazakhstan

³ Department of Intelligent Information Technologies, Ural Federal University, Yekaterinburg 620075, Russia

* Correspondence: kozlovskiy.a@inp.kz; Tel./Fax: +7-702-441-33-68

Received: 30 May 2020; Accepted: 22 June 2020; Published: 26 June 2020



Abstract: The use of nitride ceramics, in particular AlN, as structural materials for nuclear power is primarily limited by their resistance to swelling and hydrogenation processes due to the accumulation of poorly soluble helium and hydrogen ions in the structure of the surface layer. In this regard, research in this area is of great importance not only from a fundamental point of view, but also practical, since any new data on radiation resistance can make a great contribution to the development of the theory of resistance to radiation influences of structural materials of a new generation. This work is devoted to a systematic study and comparative analysis of the dynamics of radiation damage during high-dose irradiation with protons and helium ions in nitride ceramics, which have great potential for use as structural materials for GenIV reactors. The choice of irradiation doses of 1×10^{17} – 5×10^{17} ion/cm² is due to the possibility of modeling the processes of radiation damage characteristic of displacements of 10–50 dpa. During the study, the dependences of the change in the dielectric and conductive characteristics of nitride ceramics depending on the radiation dose, as well as on the type of ions, were established. The kinetics of degradation and accelerated aging was determined depending on the type of exposure. The mechanical and strength properties of ceramics were determined.

Keywords: nitride ceramics; swelling; degradation; hydrogenation

1. Introduction

The development concepts of nuclear energy and reactor engineering of the GenIV generation reactors are based on the long-term operation of structural materials under conditions of high coolant temperatures, high doses of damage (10–100 dpa), mechanical friction, and other damage [1–3]. To date, to increase the efficiency of GenIV generation reactors, it has been proposed to use higher temperatures than in WWR and WWER reactors, which reach 500–700 °C. Such temperatures make it almost impossible to use standard materials to create the first walls and protective circuits of the reactor, and requires new technical solutions and new structural materials [4,5]. In this regard, in recent decades, great attention has been paid to basic research in the field of obtaining new structural materials, as well as comprehensive study of their resistance to radiation and mechanical damage, changes in thermal conductivity, and performance at high radiation doses [6–10].

One class of prospective materials for application as a basis for structural radiation resistant materials are nitride ceramics, i.e., AlN, Si₃N₄, TiN, ZrN, etc. [11–14]. Interest in these materials is due

to high thermal conductivity, melting temperature, mechanical strength, and resistance to external effects and aggressive media.

However, in spite of the good performance of nitride ceramics, which makes them promising candidates for further use as structural materials, questions remain regarding their resistance to radiation damage, such as hydrogen disturbance and helium swelling that occurs in the surface layer of ceramics under prolonged exposure to a coolant, and exposure [15–17]. The accumulation of poorly soluble light ions in the structure can lead to their agglomeration and further formation of porous gas-filled inclusions that can result in significant degradation of the material and the formation of microcracks. Moreover, in most cases, the polycrystallinity of ceramics with several grain orientations can lead to uneven damage. In the case of large-dose irradiation of 1×10^{17} – 5×10^{17} ion/cm², according to the literature, from 0.1 to 3 at.% of implanted ions can accumulate in the ceramic structure, which leads to the formation of gas-filled bubbles, the subsequent evolution of which can have a catastrophic effect on mechanical, strength, and conductive properties of ceramics [18–20].

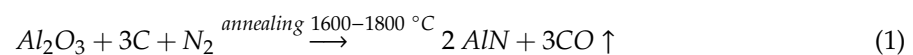
Thus, the aim of this study is to study the impacts on the change, mechanical, strength, dielectric, and conductive characteristics of nitride ceramics depending on the dose of radiation, as well as on the type of ions. In addition, special attention is paid to determining the kinetics of degradation in the simulation of accelerated aging depending on the type of exposure.

The choice of aluminum nitride from a large number of other nitride materials (Si₃N₄, TiN, BN) as the object of study is due to its high resistance to most aggressive acids, including aqua regia, HF, good thermal conductivity, high rates of mechanical strength, and insulating properties. Great interest in this type of ceramic has been shown by material scientists involved in the development of materials for the new generation of Gen IV nuclear reactors [21–23]. The high stability of aluminum nitride to the effects of heavy ions, the absence of latent ion tracks in it after irradiation, and the low mobility of grains as a result of the accumulation of defects, makes this material one of the promising materials for use as the basis for the first wall of high-temperature nuclear reactors [24,25].

The novelty of the current scientific work consists of obtaining new data on the radiation resistance of AlN ceramics to high-dose irradiation with protons and helium ions and subsequent aging, as well as changes in properties due to external influences. As a rule, irradiation with doses higher than 1 – 3×10^{17} ion/cm² is considered the initial dose of the initialization of the processes of blister formation and swelling of ceramic materials, which leads to an acceleration of degradation processes.

2. Experimental Part

The object of the study was polycrystalline ceramics based on aluminum nitride (AlN) (see Figure 1a,b) with a hexagonal-type crystal structure and three main texture orientations: (100), (002), and (101). According to the method of production by sintering ceramics in an atmosphere of nitrogen (N₂) (P = 760 mmHg) from alumina powders:



According to X-ray data, impurity inclusions of alumina remained in the ceramic structure, the concentration of which did not exceed 3–4%. The density of ceramics according to the passport data and X-ray diffraction analysis was 3.25–3.26 g/cm³, which is in good agreement with the density data for this type of ceramics. As a stabilizing additive, Y₂O₃ powder was used. The presence of oxide inclusions in the structure also led to an increase in the stability of nitride ceramics and, according to previous studies, these impurity inclusions have an isotropic distribution over the entire volume [26,27].

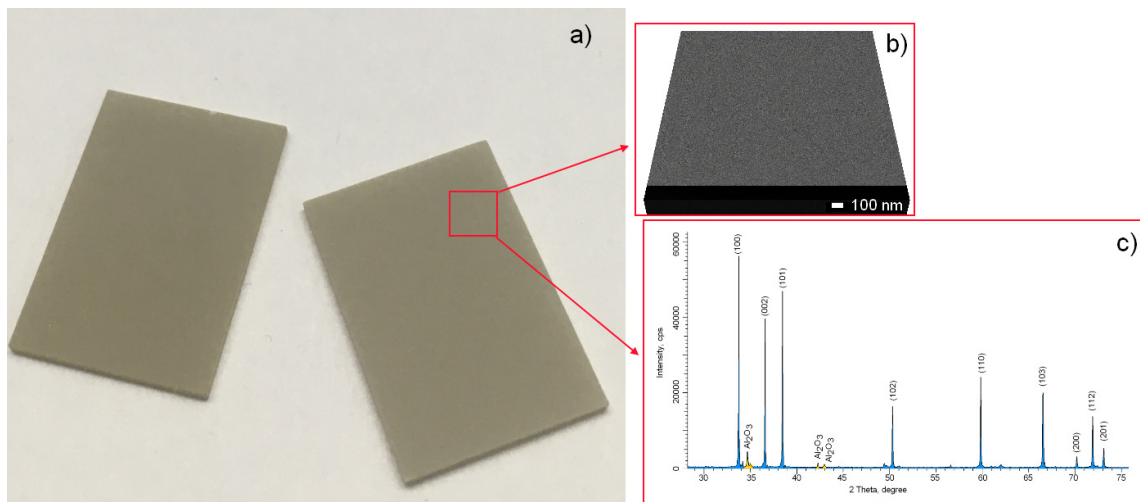


Figure 1. (a) Appearance of the original ceramics; (b) SEM image of the morphology of the original sample; (c) typical X-ray diffraction pattern of polycrystalline ceramic of aluminum nitride with a hexagonal type crystal lattice and impurity oxide inclusions.

Ceramics were irradiated with the aim of modeling hydrogenation and helium swelling processes with two types of ions: (1) protons with an energy of 500 keV, the mean free path of which, according to the SRIM Pro 2013 program code (srim.org) [28], was $4.1 \pm 0.2 \mu\text{m}$; and 2) helium ions with an energy of 40 keV and path length of 400–500 nm. The radiation doses were 1×10^{17} – 5×10^{17} ion/cm², which, according to the conversion to the atomic displacements (dpa), was 10–50 dpa. The concentration of implanted ions was calculated by Formula (2):

$$C_{ion} = \sigma\Phi, \quad (2)$$

where σ is the total cross section for defect formation in the case of irradiation with various ions, and Φ is the irradiation fluence.

The study of dielectric loss was carried out using the method of impedance spectroscopy performed on a HIOKI IM 3570 Impedance Analyzer, (Koizumi, Ueda, Nagano, Japan).

Thermal conductivity was measured using the stationary method of measuring the absolute longitudinal heat flux proposed in [29]. The coefficient of thermal conductivity was determined using Formula (3):

$$\lambda = \frac{q\delta}{t_{c1} - t_{c2}} \quad (3)$$

where q is the heat flux density, W/m²; t_{c1} and t_{c2} are the temperature constants on the hot and cold sides of the wall, respectively, K; δ is the wall thickness, m; λ is the coefficient of thermal conductivity of the wall material, W/(m·K) [26]. The range of t_{c1} and t_{c2} as a result of thermal conductivity tests ranged from 300 to 1000 K. Ten independent measurements were made for each test sample.

The dynamics of changes in the morphology of the surface of ceramics before and after irradiation were studied using the scanning electron microscopy method performed using a “Hitachi TM3030” microscope (Hitachi Ltd., Chiyoda, Tokyo, Japan) with the following settings: Shooting mode—LEI, Current—20 μA , Accelerate voltage—2 kV, WD = 8 mm.

The kinetics of the degradation of ceramics before and after irradiation in the case of low-temperature degradation of the surface microstructure as a result of irradiation and aging, under accelerated degradation, was studied using the method of modeling the external effects of water vapor at a temperature of 150 °C and a pressure of 2.2–2.3 atm. Using these conditions for modeling aging and degradation processes allows accelerating the natural aging process, which takes years to complete. In the case of modeling, 1 hour of treatment is equivalent to 1.5–2.0 years of aging in vivo.

3. Results and Discussion

Figure 2 presents the results of changes in the surface morphology of irradiated ceramics with doses of 5×10^{17} ion/cm², obtained using scanning electron microscopy.

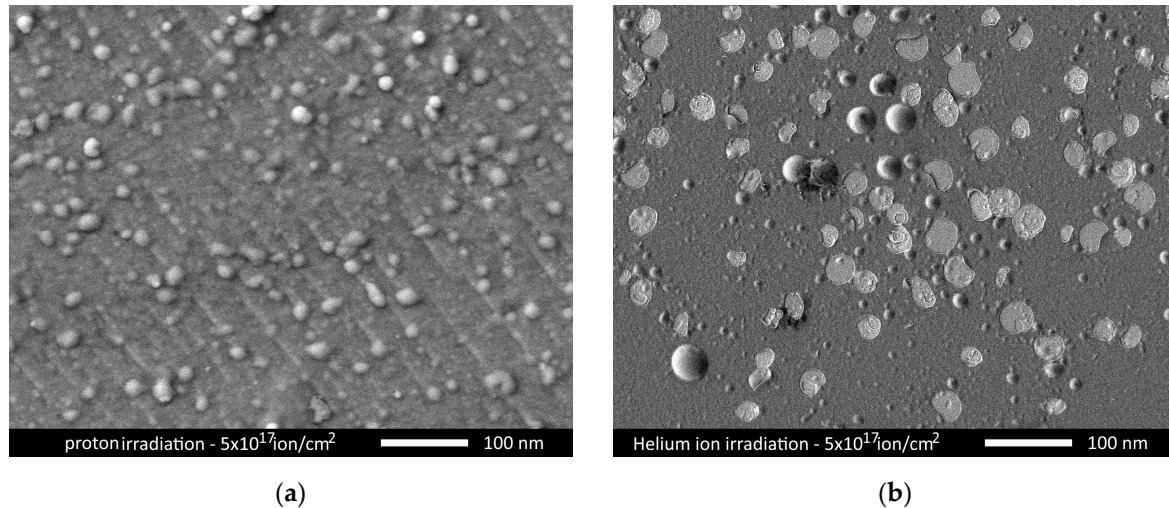


Figure 2. SEM images of morphological changes in the surface of ceramics after irradiation with a dose of 5×10^{17} ion/cm² by (a) protons and (b) helium ions.

As can be seen from the data presented, in the case of proton irradiation on the surface of ceramics, the formation of spherical inclusions is observed, the average size of which does not exceed 10–15 nm (see Figure 3). These inclusions are gas-filled bubbles resulting from implantation and subsequent agglomeration of hydrogen or helium in the structure of the surface layer. The mechanism of bubble formation is as follows. When irradiated with low-energy particles, the path length of which ranges from 300 nm to 3–5 μ m, the main energy losses causing drag are inelastic collisions with nuclei, which lead to distortions and deformations of the crystal lattice, most of which annihilate in a short period of time. In this case, the remaining part of the formed defects is able to begin to migrate along the structure, thereby introducing additional deformation effects as a result of cascading collisions. In the case of large radiation doses of 1×10^{17} – 5×10^{17} ion/cm², a large number of overlapping cascade defects are observed during the interaction of ions with the crystal structure of the irradiated target, which can be from 1000 to 100,000 overlaps [30]. It is also worth noting that, in the case of protons and helium ions, in view of their weak solubility and great ability to implant, and subsequent agglomeration near grain boundaries, at high radiation doses voids filled with gas can form in the structure, as well as strongly deformed regions. Due to their nature, these can be squeezed to the surface as a result of overstresses and deformations of the crystal structure. Moreover, in the case of irradiation with helium ions, not only does the size of the bubbles increase, but most are destroyed, which indicates a partial degradation of the surface layer. The presence of craters from exploding bubbles, as well as smaller bubbles, indicates swelling and embrittlement of the surface layer as a result of the accumulation of implanted helium at high radiation doses, which amounted to 3.7% for the maximum radiation dose.

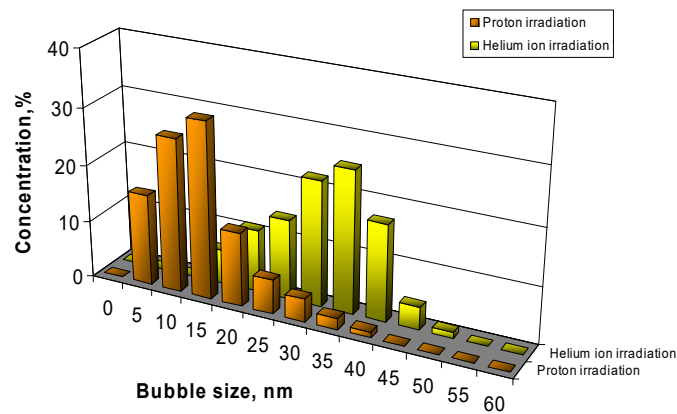


Figure 3. Diagram of changes in the size of gas bubbles on the surface of ceramics at an irradiation dose of 5×10^{17} ion/cm².

Figure 4 shows the results of the effect of irradiation on the change in the dielectric properties of ceramics depending on the dose of radiation and the type of exposure.

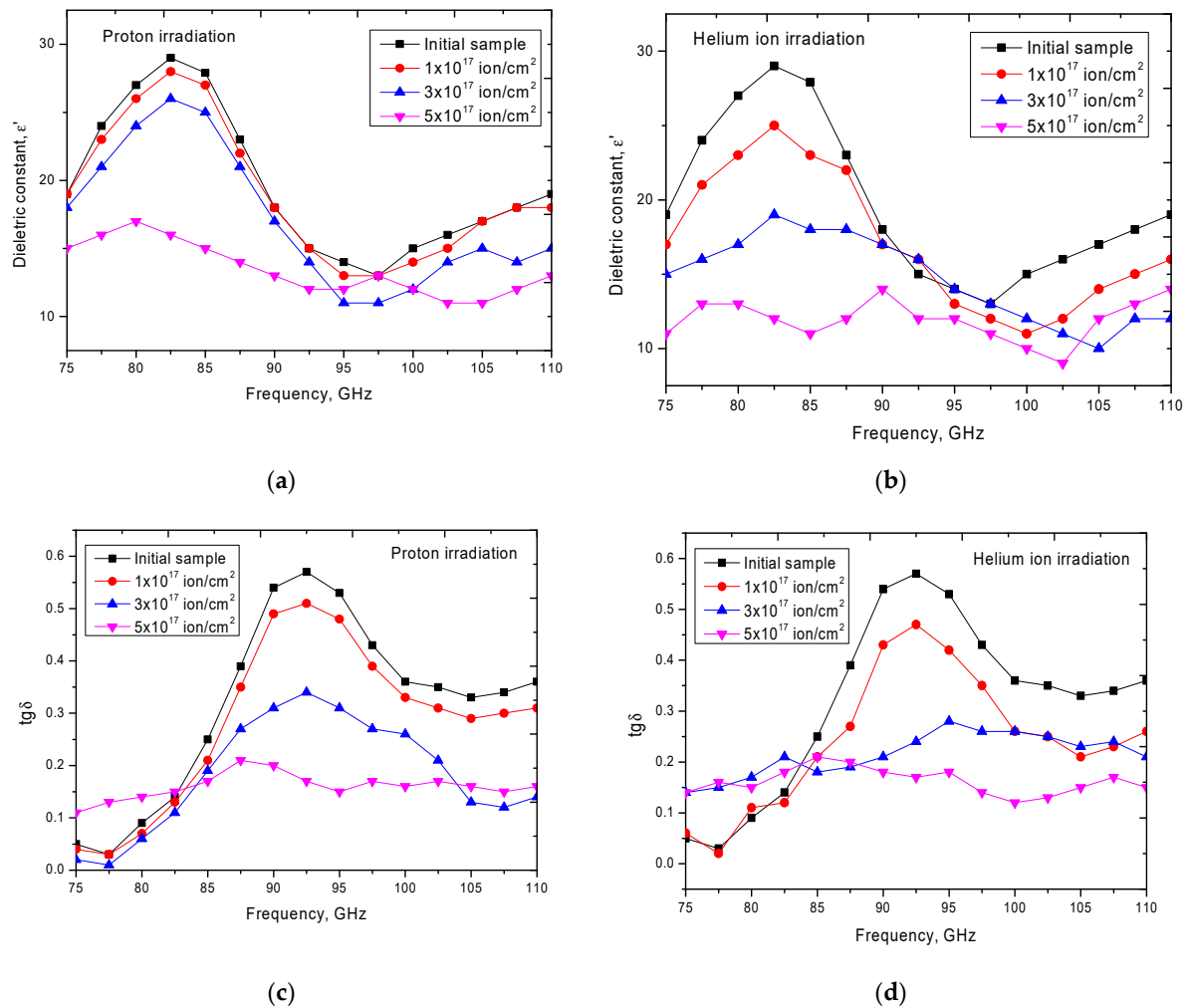


Figure 4. Graphs of the dependence of the dielectric constant on the type of exposure: (a) proton irradiation; (b) helium ion irradiation; and dielectric loss ($\text{tg}\delta$): (c) proton irradiation (d) helium ion irradiation.

The study of the dielectric properties of ceramics exposed to radiation is due to the fact that these ceramics can be used not only as materials for the first wall of nuclear reactors for which thermal conductivity and crack resistance are one of the most important characteristics, but also as the basis for substrates or printed circuit boards of microelectronic circuits, working in conditions of increased radiation background.

According to the data presented, in the case of proton irradiation, the values of the dielectric constant and dielectric loss practically do not change at irradiation doses of 1×10^{17} – 3×10^{17} ion/cm², which indicates a small effect of the formed defects upon irradiation on the dielectric properties. However, the appearance of voids and gas-filled bubbles at an implanted hydrogen concentration of 1.7–1.8% at an irradiation dose of 5×10^{17} ion/cm² leads to deterioration in the dielectric properties of ceramics and their degradation. In the case of irradiation with helium ions, the degradation of dielectric properties is observed for a fluence of 3×10^{17} ion/cm² and higher, which is also due to the degradation of ceramics due to swelling during the accumulation of defects in the structure.

Figure 5 shows the dynamics of changes in the coefficient of thermal conductivity, which characterizes the heat-conducting properties of the material and is one of the most important operational characteristics of ceramics, the change of which can have a significant negative impact on the performance of reactors.

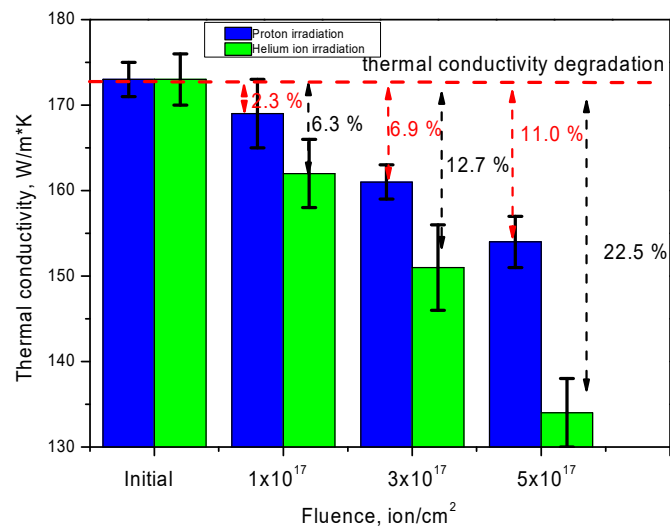


Figure 5. Diagram of the dependence of the coefficient of thermal conductivity on the dose and type of exposure.

As can be seen from the data presented, in the case of proton irradiation and the accumulation of defects in the structure of ceramics as a result of hydrogenation, the maximum thermal conductivity is reduced at a dose of 5×10^{17} ion/cm² by no more than 11% of the initial value. However, the occurrence of helium inclusions in the structure and a high concentration of defects lead to a sharp deterioration in heat dissipation and a decrease in the thermal conductivity by an amount exceeding 20% at the maximum radiation dose.

The results of studying the kinetics of ceramic degradation under accelerated aging of initial and irradiated samples are presented below (see Figure 6). Kinetics was determined by measuring the crack resistance of ceramics after a certain time. According to the data obtained, for the initial sample, there is a slight decrease in crack resistance in the range of 5–7% for the entire test period, which is comparable in time to 50–60 years. The technique of low-temperature aging under the influence of water vapor under pressure is one of the common methods capable of simulating the effect of aging of ceramics. This technique has established itself as one of the most effective and accurate methods of artificial aging of materials due to external influences [31–33]. Ten measurements were made for each test sample.

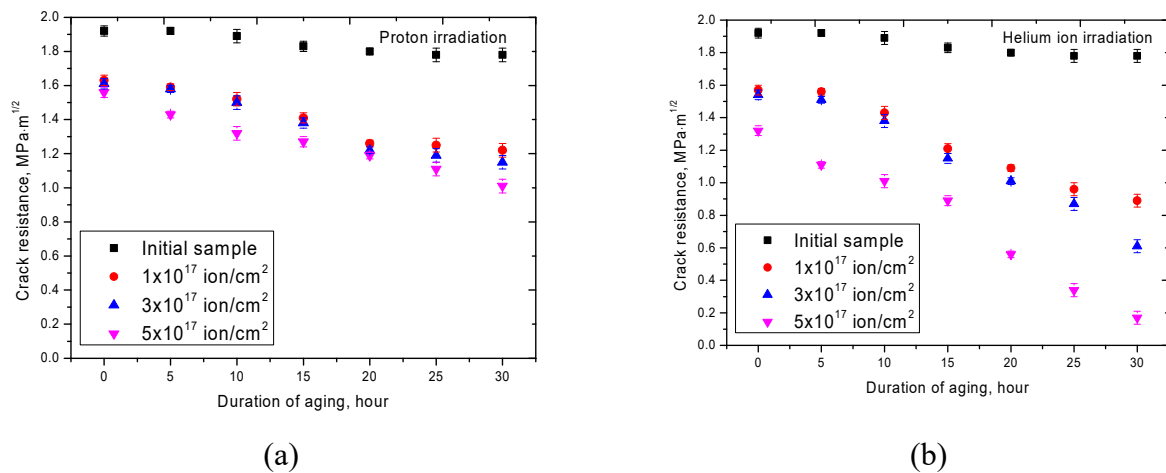


Figure 6. Graphs of the dependence of the crack resistance on the aging time of the samples: (a) proton irradiation; (b) helium ion irradiation.

The small value of sample degradation in the initial state indicates a high resistance of ceramics to aging and embrittlement. For proton-irradiated samples, a decrease in crack resistance by 15–19% is observed compared with the initial sample, however, an increase in fluence does not lead to significant differences in the decrease in crack resistance. During aging tests, the decrease in crack resistance for proton-irradiated samples occurs in two stages. The first stage is characterized by a gradual decrease in crack resistance for cases of irradiation of 1×10^{17} – 3×10^{17} ion/cm². The second stage is characterized by an almost constant value of crack resistance, which indicates the stabilization of the crack resistance and the absence of mechanisms for further destruction of the structure. However, for irradiated samples with a fluence of 5×10^{17} ion/cm², the decrease in crack resistance is constant over the course of the test time. In the case of ceramics irradiated with helium ions, for fluxes of irradiation of 1×10^{17} – 3×10^{17} ion/cm², a decrease in the crack resistance is observed comparable with irradiation with protons, and an increase in fluence to 5×10^{17} ion/cm² leads to a decrease in the value by 35–37% from the initial value. In this case, in contrast to proton irradiation, for which the decrease in crack resistance over time ranges from 25 to 45% depending on the dose, for samples irradiated with helium ions, the decrease in crack resistance after the test time ranges from 25 to 87% depending on the dose exposure (see chart data in Figure 7).

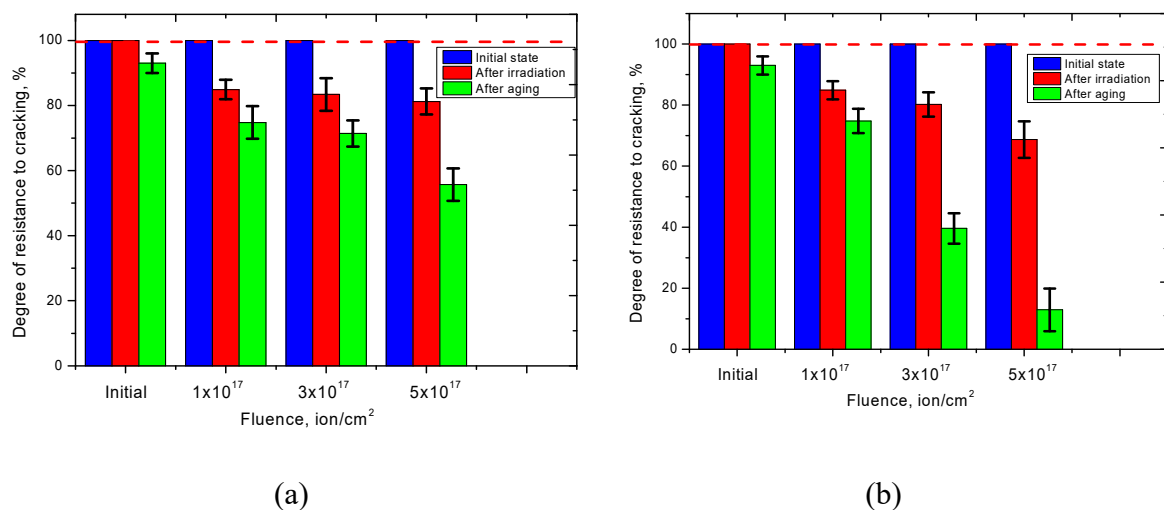


Figure 7. Diagram of the dependence of changes in the degree of resistance to cracking: (a) proton irradiation; (b) helium ion irradiation.

Figure 8 presents the results of changes in the morphology of ceramics in the initial state and irradiated with a dose of 5×10^{17} ion/cm² after 30 h of aging.

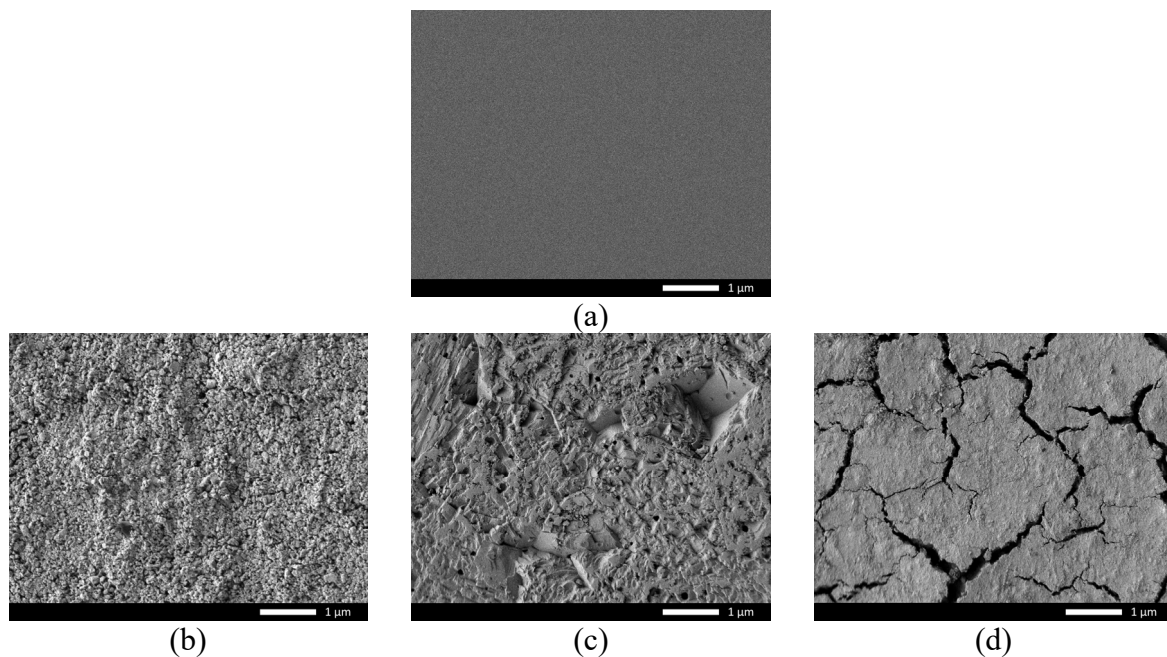


Figure 8. SEM images of ceramic: (a) initial sample; (b) initial sample after aging; (c) proton irradiation after aging; (d) helium ion irradiation after aging.

In the case of the initial sample, aging leads to crushing of grains and a significant increase in surface roughness due to the formation of a fine-grained structure. For proton-irradiated samples, the aging effect has a catastrophic effect on the degradation of the surface layer, with the formation of porous cells and microcracks characteristic of ulcerative corrosion. For samples irradiated with helium ions, the formation of large branched cracks indicates partial destruction as a result of structural degradation.

To describe the effects of irradiation and aging, one can propose the following mechanism of surface layer degradation. When irradiated with helium ions or protons, regions with a high degree of disorder are formed in the structure of the surface layer at various depths, which arise both as a result of elastic and inelastic collisions of incident particles with electron shells (elastic interactions) and target nuclei (inelastic interactions), and as a result of the formation of cascading effects of the migration of point defects and initially knocked out atoms. Moreover, in the case of proton irradiation, the probability of the formation of initially knocked out atoms is small due to the small size of the incident particles, as well as large energy losses on the electron shells with the subsequent formation of cascades of knocked out electrons. In the case of irradiation with low-energy helium ions, inelastic collisions predominate, which can lead to the displacement of atoms from the lattice sites, and thereby significantly increase the degree of deformation of the crystal structure. Furthermore, due to the high penetrating ability of protons in ceramics and a significantly larger mean free path (4 μm), the density of defects in the near-surface layer 300–500 nm thick is much lower than when irradiated with helium ions. In this regard, for samples irradiated with helium ions, the surface layer (300–500 nm) is subject to great deformation not only due to the large number of defects formed, but also helium bubbles that form at high doses of radiation, inside which additional pressure accumulates, leading to bloating bubbles. When modeling the effects of aging of ceramics irradiated with protons, the surface layer of which contains fewer defects than a similar layer of ceramics irradiated with helium ions, the degradation of the layer occurs due to the destruction of the disordering regions and partial cracking of the irradiated layer with the formation of a porous structure, which indicates the presence of irradiated samples gas-filled inclusions of small size (5–15 nm). For samples irradiated with helium ions, in the surface

layer of which, at high radiation doses, strongly distorted defective regions and blisters are formed, explosive destruction of gas-filled bubbles occurs with increasing exposure time of the vapor, with the formation of microcracks along the grain boundaries that serve as defect sinks.

Thus, it was found that, at an irradiation dose of 5×10^{17} ion/cm² characteristic of a displacement of 50 dpa, the degradation of the surface layer of ceramics is catastrophic in nature, which can have a significant impact on the performance characteristics of structural materials.

The data obtained are in good agreement with the previously presented studies on the radiation resistance to helium embrittlement and swelling of nitride materials. For example, data on resistance to the formation of blisters and helium bubbles have a good correlation with similar results for thin-film multilayer coatings based on ZrN, CrN, and AlN [34,35]. The authors of these works found that the degradation of nitride materials as a result of the accumulation of implanted helium occurs as a result of the formation of porous inclusions and deformations of the structure of the surface layer at low irradiation fluences. An increase in the irradiation fluence leads to the filling of these cavities with poorly soluble helium ions, followed by the formation of helium bubbles. Moreover, for different samples, the dose loads necessary to start the nucleation of bubbles are different. In the case of proton irradiation with nitride ceramics, the structural changes resulting from the irradiation are in good agreement with previous work [36–39], according to which it was found that, in the case of large-dose irradiation, the main structural changes are associated with the formation of microcracks and disordering regions. In this case, the presence of impurities of other elements in the structure of nitride ceramics leads to the formation of additional disordering regions and accumulations of defects.

4. Conclusions

The paper presents the comparative results of the influence of large-dose irradiation with protons and helium ions on the properties of nitride ceramics, as well as the kinetics of degradation due to aging. It was established that for nitride ceramics, irradiation with helium ions at a dose of 5×10^{17} ion/cm² leads to large effects of degradation and swelling as a result of the accumulation of helium bubbles in the structure of the surface layer. For both types of irradiation, it was found that a dose of 5×10^{17} ion/cm² has a significant negative effect on the dielectric properties, the decrease of which is due to the occurrence of distortions and gas-filled voids in the structure of ceramics. In the course of life aging tests, it was found that in the case of proton irradiation, the decrease in crack resistance is in the range of 25–45% of the initial value depending on the radiation dose, and for samples irradiated with helium ions, the decrease in crack resistance ranges from 25 to 87%, depending on radiation doses. Moreover, the mechanisms of degradation of irradiated ceramics are different.

Author Contributions: Conceptualization, M.V.Z., D.I.S., D.B.B., I.E.K. and A.L.K.; methodology, D.I.S., D.B.B., I.E.K. and A.L.K.; formal analysis, M.V.Z.; investigation, D.I.S., I.E.K., A.L.K., and M.V.Z.; resources, M.V.Z.; writing—original draft preparation, review and editing, D.I.S., D.B.B., I.E.K., M.V.Z., and A.L.K.; visualization, M.V.Z.; supervision, M.V.Z. All authors have read and agreed to the published version of the manuscript.

Funding: This research was funded by the Science Committee of the Ministry of Education and Science of the Republic of Kazakhstan (No. AP08051975).

Conflicts of Interest: The authors declare that they have no conflict of interest.

References

1. Khafizov, M.; Chauhan, V.; Wang, Y.; Riyad, F.; Hang, N.; Hurley, D.H. Investigation of thermal transport in composites and ion beam irradiated materials for nuclear energy applications. *J. Mater. Res.* **2017**, *32*, 204–216. [[CrossRef](#)]
2. Zinkle, S.J. Advanced irradiation-resistant materials for Generation IV nuclear reactors. In *Structural Materials for Generation IV Nuclear Reactors*; Woodhead Publishing: Sawston, UK, 2017; pp. 569–594.
3. Kong, X.; Fu, Z.; Que, H.; Fan, Y.; Chen, Z.; He, C. Effects of recording time and residue on dose-response by LiMgPO₄: Tb, B ceramic disc synthesized via improved sintering process. *Nucl. Instrum. Methods Phys. Res. Sect. B Beam Interact. Mater. At.* **2018**, *422*, 12–17. [[CrossRef](#)]

4. Aitkaliyeva, A.; He, L.; Wen, H.; Miller, B.; Bai, X.M.; Allen, T. Irradiation effects in Generation IV nuclear reactor materials. In *Structural Materials for Generation IV Nuclear Reactors*; Woodhead Publishing Series in Energy: Sawston, UK, 2017; pp. 253–283.
5. Murty, K.L.; Charit, I. Structural materials for Gen-IV nuclear reactors: Challenges and opportunities. *J. Nucl. Mater.* **2008**, *383*, 189–195. [[CrossRef](#)]
6. Locatelli, G.; Mancini, M.; Todeschini, N. Generation IV nuclear reactors: Current status and future prospects. *Energy Policy* **2013**, *61*, 1503–1520. [[CrossRef](#)]
7. Klym, H.; Ingram, A.; Shpotyuk, O.; Hadzaman, I.; Solntsev, V.; Hotra, O.; Popov, A.I. Positron annihilation characterization of free volume in micro-and macro-modified CuO. 4CoO. 4NiO. 4Mn1. 8O4 ceramics. *Low Temp. Phys.* **2016**, *42*, 601–605. [[CrossRef](#)]
8. Yano, T.; Ichikawa, K.; Akiyoshi, M.; Tachi, Y. Neutron irradiation damage in aluminum oxide and nitride ceramics up to a fluence of $42 \times 10^{26} \text{ n/m}^2$. *J. Nucl. Mater.* **2000**, *283*, 947–951. [[CrossRef](#)]
9. Garcia, C.B.; Brito, R.A.; Ortega, L.H.; Malone, J.P.; McDeavitt, S.M. Manufacture of a UO₂-Based Nuclear Fuel with Improved Thermal Conductivity with the Addition of BeO. *Metall. Mater. Trans.* **2017**, *E.4*, 70–76.
10. Lushchik, A.; Lushchik, C.; Popov, A.I.; Schwartz, K.; Shablonin, E.; Vasil'chenko, E. Influence of complex impurity centres on radiation damage in wide-gap metal oxides. *Nucl. Instrum. Methods Phys. Res. Sect. B Beam Interact. Mater. At.* **2016**, *374*, 90–96. [[CrossRef](#)]
11. Li, Y.; Gao, J. Preparation of silicon nitride ceramic fibers from polycarbosilane fibers by γ -ray irradiation curing. *Mater. Lett.* **2013**, *110*, 102–104. [[CrossRef](#)]
12. Zhukovskii, Y.F.; Pugno, N.; Popov, A.I.; Balasubramanian, C.; Bellucci, S. Influence of F centres on structural and electronic properties of AlN single-walled nanotubes. *J. Phys. Condens. Matter* **2007**, *19*, 395021. [[CrossRef](#)]
13. Yano, T.; Inokuchi, K.; Shikama, M.; Ukai, J.; Onose, S.; Maruyama, T. Neutron irradiation effects on isotope tailored aluminum nitride ceramics by a fast reactor up to $2 \times 10^{26} \text{ n/m}^2$. *J. Nucl. Mater.* **2004**, *329*, 1471–1475. [[CrossRef](#)]
14. Yano, T.; Iseki, T. Swelling and microstructure of AlN irradiated in a fast reactor. *J. Nucl. Mater.* **1993**, *203*, 249–254. [[CrossRef](#)]
15. Nigam, S.; Kim, J.; Ren, F.; Chung, G.Y.; MacMillan, M.F.; Dwivedi, R.; Pearton, S.J. High energy proton irradiation effects on SiC Schottky rectifiers. *Appl. Phys. Lett.* **2002**, *81*, 2385–2387. [[CrossRef](#)]
16. Wakai, E.; Hashimoto, N.; Miwa, Y.; Robertson, J.P.; Klueh, R.L.; Shiba, K.; Jistikawa, S. Effect of helium production on swelling of F82H irradiated in HFIR. *J. Nucl. Mater.* **2000**, *283*, 799–805. [[CrossRef](#)]
17. Leclerc, S.; Declémy, A.; Beaufort, M.F.; Tromas, C.; Barbot, J.F. Swelling of SiC under helium implantation. *J. Appl. Phys.* **2005**, *98*, 113506. [[CrossRef](#)]
18. Kotomin, E.A.; Kuzovkov, V.N.; Popov, A.I. The kinetics of defect aggregation and metal colloid formation in ionic solids under irradiation. *Radiat. Eff. Defects Solids* **2001**, *155*, 113–125. [[CrossRef](#)]
19. Yamaguchi, M.; Taylor, S.J.; Yang, M.J.; Matsuda, S.; Kawasaki, O.; Hisamatsu, T. High-energy and high-fluence proton irradiation effects in silicon solar cells. *J. Appl. Phys.* **1996**, *80*, 4916–4920. [[CrossRef](#)]
20. Yutani, K.; Kishimoto, H.; Kasada, R.; Kimura, A. Evaluation of Helium effects on swelling behavior of oxide dispersion strengthened ferritic steels under ion irradiation. *J. Nucl. Mater.* **2007**, *367*, 423–427. [[CrossRef](#)]
21. Onoda, Y.; Kimura, H.; Kato, T.; Fukuda, K.; Kawaguchi, N.; Yanagida, T. Thermally stimulated luminescence properties of Eu-doped AlN ceramic. *Optik* **2019**, *181*, 50–56. [[CrossRef](#)]
22. Patino, M.I.; Doerner, R.P.; Tynan, G.R. Exposure of AlN and Al₂O₃ to low energy D and He plasmas. *Nucl. Mater. Energy* **2020**, 100753. [[CrossRef](#)]
23. Sall, M.; Moisy, F.; Mattei, J.G.; Grygiel, C.; Balanzat, E.; Monnet, I. Electronic excitations induced climb of dislocations in swift heavy ion irradiated AlN and Al_xGa_{1-x}N. *Nucl. Instrum. Methods Phys. Res. Sect. B Beam Interact. Mater. At.* **2018**, *435*, 116–120. [[CrossRef](#)]
24. Zinkle, S.J.; Hodgson, E.R. Radiation-induced changes in the physical properties of ceramic materials. *J. Nucl. Mater.* **1992**, *191*, 58–66. [[CrossRef](#)]
25. Zinkle, S.J.; Kinoshita, C. Defect production in ceramics. *J. Nucl. Mater.* **1997**, *251*, 200–217. [[CrossRef](#)]
26. Kozlovskiy, A.; Dukenbayev, K.; Kenzhina, I.; Tosi, D.; Zdorovets, M. Dynamics of changes in structural properties of AlN ceramics after Xe⁺ 22 ion irradiation. *Vacuum* **2018**, *155*, 412–422. [[CrossRef](#)]
27. Gladkikh, T.; Kozlovskiy, A.; Kenzhina, I.; Dukenbayev, K.; Zdorovets, M. Changes in optical and structural properties of AlN after irradiation with C²⁺ ions of 40 keV. *Vacuum* **2019**, *161*, 103–110. [[CrossRef](#)]

28. Biersack, J.P.; Haggmark, L.G. A Monte Carlo computer program for the transport of energetic ions in amorphous targets. *Nucl. Instrum. Methods* **1980**, *174*, 257–269. [[CrossRef](#)]
29. Yang, B.; Liu, J.L.; Wang, K.L.; Chen, G. Simultaneous measurements of Seebeck coefficient and thermal conductivity across superlattice. *Appl. Phys. Lett.* **2002**, *80*, 1758–1760. [[CrossRef](#)]
30. Wesch, W.; Wendler, E. *Ion Beam Modification of Solids*; Springer Nature: Cham, Switzerland, 2016; Volume 61.
31. Zhigachev, A.O.; Umrikhin, A.V.; Korenkov, V.V.; Golovin, Y.I. Low-temperature aging of baddeleyite-based Ca-TZP ceramics. *J. Am. Ceram. Soc.* **2017**, *100*, 3283–3292. [[CrossRef](#)]
32. Pereira, G.K.R.; Venturini, A.B.; Silvestri, T.; Dapieve, K.S.; Montagner, A.F.; Soares, F.Z.M.; Valandro, L.F. Low-temperature degradation of Y-TZP ceramics: A systematic review and meta-analysis. *J. Mech. Behav. Biomed. Mater.* **2016**, *55*, 151–163. [[CrossRef](#)]
33. Pereira, G.K.R.; Silvestri, T.; Camargo, R.; Rippe, M.P.; Amaral, M.; Kleverlaan, C.J.; Valandro, L.F. Mechanical behavior of a Y-TZP ceramic for monolithic restorations: Effect of grinding and low-temperature aging. *Mater. Sci. Eng.* **2016**, *C 63*, 70–77. [[CrossRef](#)]
34. Uglov, V.V.; Abadias, G.; Zlotski, S.V.; Saladukhin, I.A.; Malashevich, A.A.; Kozlovskiy, A.L.; Zdorovets, M.V. Blistering in Helium-Ion-Irradiated Zirconium, Aluminum, and Chromium Nitride Films. *J. Surf. Investig. X-ray Synchrotron Neutron Tech.* **2020**, *14*, 359–365. [[CrossRef](#)]
35. Uglov, V.V.; Abadias, G.; Zlotski, S.V.; Saladukhin, I.A.; Cherenda, N.N. Surface blistering in ZrSiN nanocomposite films irradiated with He ions. *Surf. Coat. Technol.* **2020**, *394*, 125654. [[CrossRef](#)]
36. ves, N.E.; Chen, J.; Witulski, A.F.; Schrimpf, R.D.; Fleetwood, D.M.; Bruce, R.W.; Massengill, L.W. Effects of proton-induced displacement damage on gallium nitride HEMTs in RF power amplifier applications. *IEEE Trans. Nucl. Sci.* **2015**, *62*, 2417–2422. [[CrossRef](#)]
37. Kim, H.Y.; Ahn, J.; Kim, J.H.; Yun, S.P.; Lee, J.S. Characterization of AlGaIn/GaN HEMT irradiated at 5 keV and 25 MeV proton energies. *J. Ceram. Process. Res.* **2008**, *9*, 155–157.
38. Dukenbayev, K.; Kozlovskiy, A.; Alyamova, Z.A.; Gladkikh, T.; Kenzhina, I.; Zdorovets, M. The investigation of various type irradiation effects on aluminum nitride ceramic. *J. Mater. Sci. Mater. Electron.* **2019**, *30*, 8777–8787. [[CrossRef](#)]
39. Gan, J.; Yang, Y.; Dickson, C.; Allen, T. Proton irradiation study of GFR candidate ceramics. *J. Nucl. Mater.* **2009**, *389*, 317–325. [[CrossRef](#)]

